ADVANCED MATERIALS

Supporting Information

for *Adv. Mater.,* DOI: 10.1002/adma.201501030

Ultrahigh Thermoelectric Performance in Mosaic Crystals

Ying He, Ping Lu, Xun Shi, Fangfang Xu,* Tiansong Zhang, Gerald Jeffrey Snyder, Ctirad Uher, and Lidong Chen**

Supporting Information

Title Ultrahigh Thermoelectric Performance in Mosaic Crystals

Ying He[1,2,3], Ping Lu[1,3], Xun Shi[1,2,], Fangfang Xu[1,]*,Tiansong Zhang[2], G. Jeffrey Snyder[4], Ctirad Uher[5] and Lidong Chen[1,2,]**

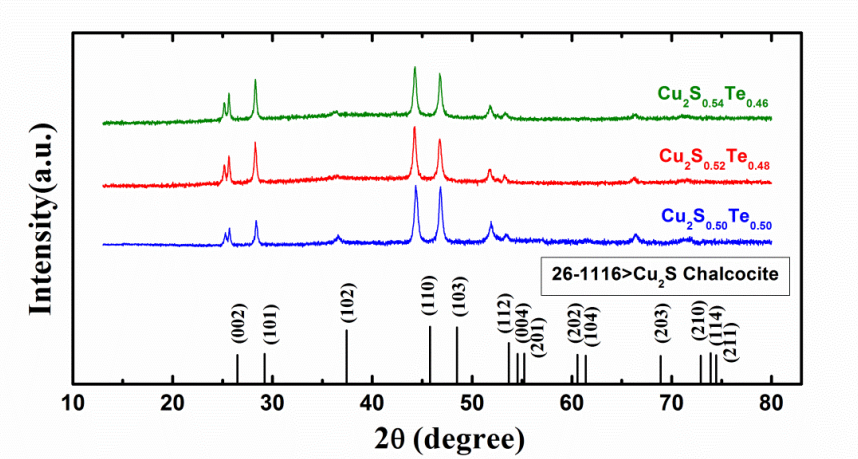

Figure S1. XRD measurement of $Cu_2(S, Te)$ solid solutions. The diffraction peaks match with the hexagonal Cu_2S (between 370K and 710K) having a space group P 6_3/mmc. As the ionic radius of Te is much larger than that of S, all diffraction peaks move toward lower angles.

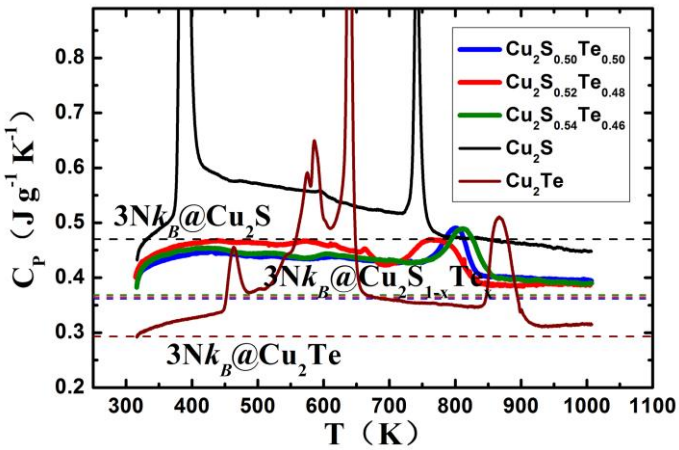

Figure S2. Temperature dependence of heat capacity of pure Cu_2S,[13] Cu_2Te and mosaic crystals of $Cu_2(S, Te)$. The dashed lines represent the theoretical values of $3Nk_B$.

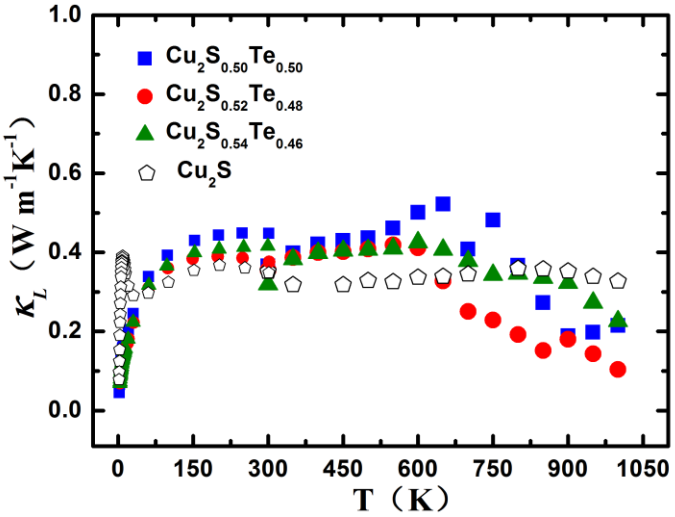

Figure S3. Temperature dependence of the lattice thermal conductivity of Cu_2(S, Te) mosaic crystals.

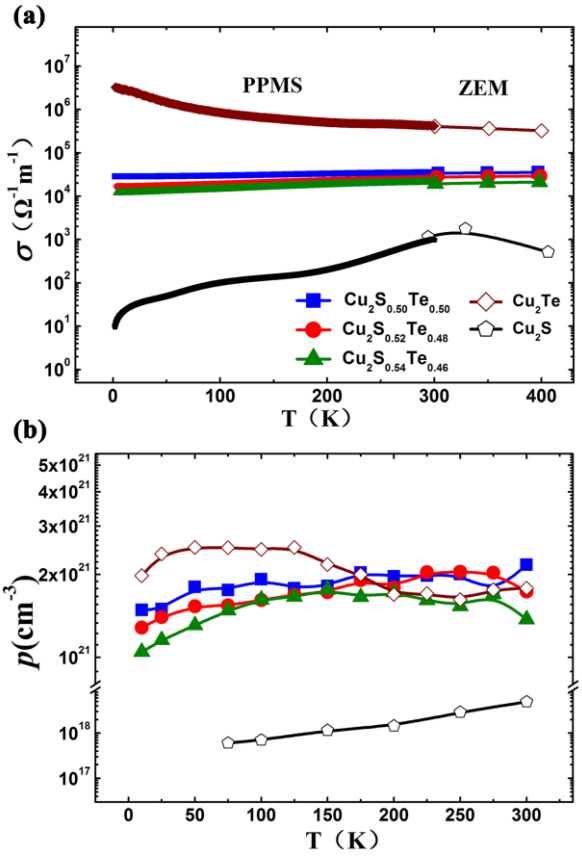

Figure S4. Temperature dependence of electronic transport parameters at low temperatures. (a) Electrical conductivity. (b) Carrier concentration.

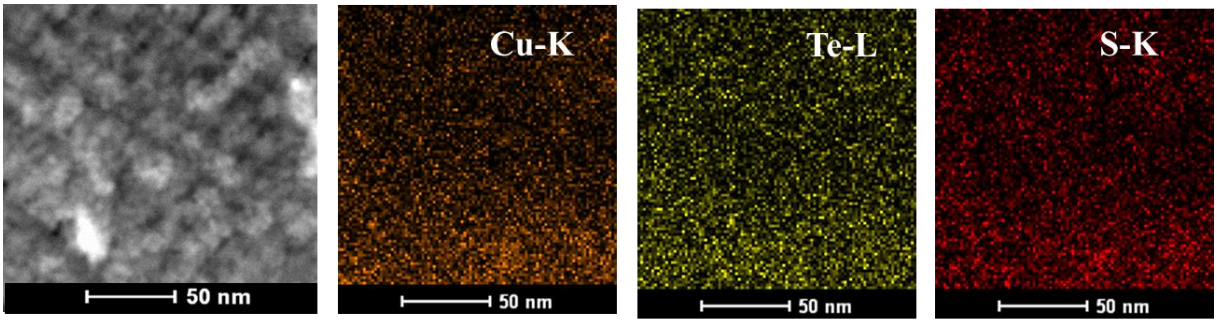

Figure S5. Element mapping from EDS measurements in TEM.

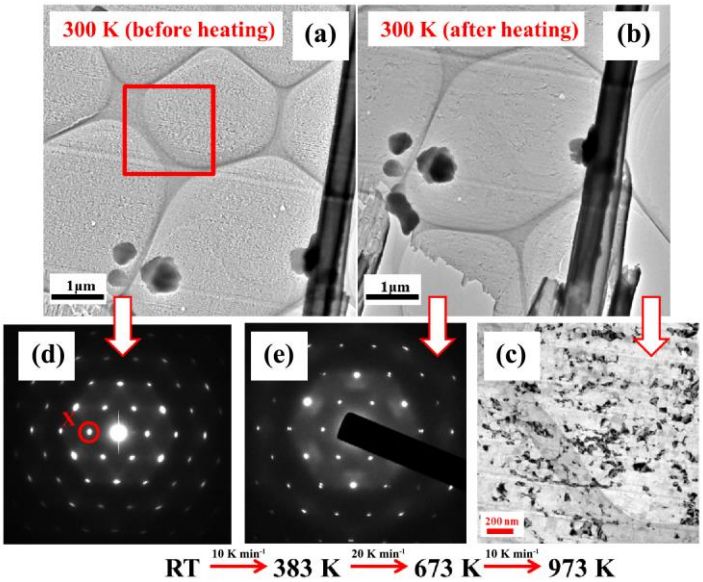

Figure S6. (a) TEM bright-field image of an ultrathin sectioned $Cu_2(S, Te)$ sample. **(b)** TEM micrograph of the same area as in Figure S6(a) taken at room temperature after the sample cooled from 973K. **(c)** Enlarged image from an area in Figure S6(b) showing coarsened mosaic grains. **(d)** and **(e)** Electron diffraction patterns corresponding to Figure S6(a) and Figure S6(b), respectively. They show nearly identical patterns, suggesting the maintenance of mosaic crystals after heating the samples.

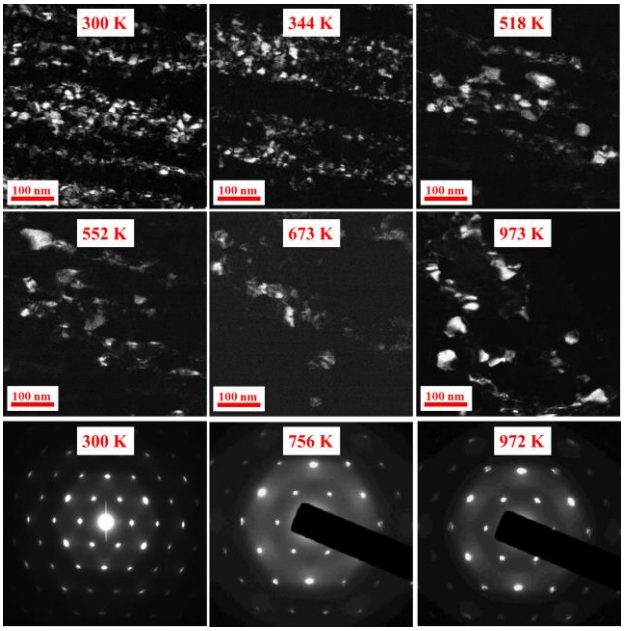

Figure S7. Evolution of mosaic structures upon heating. Images are acquired using the reflection marked as X in Figure S6(d) at high temperatures.

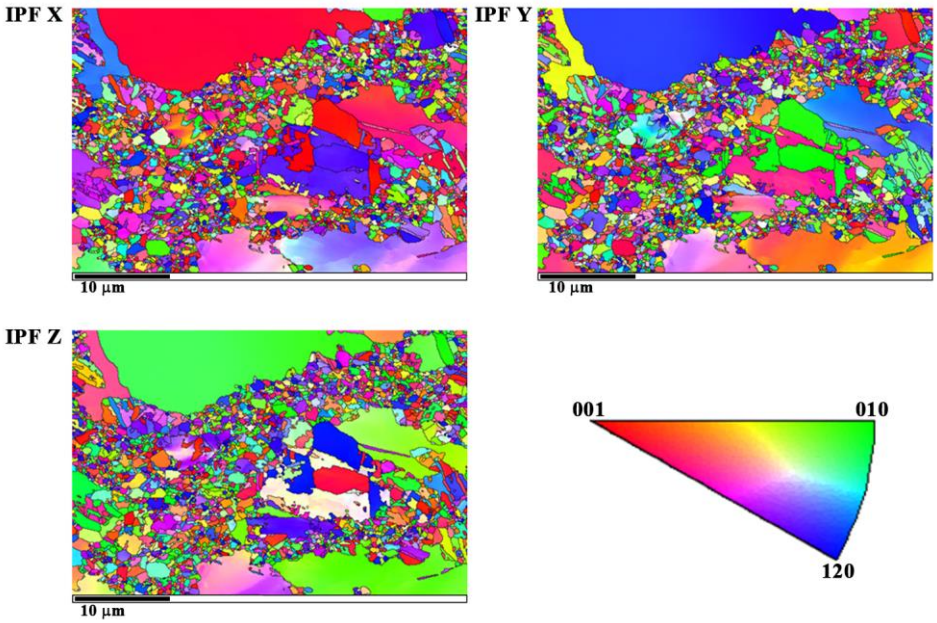

Figure S8. Grain orientation distribution in the inverse pole figure (IPF) at three direction by EBSD (Electron Backscatter Diffraction) measurement.